

FULL WAVEFORM MODELING OF THE EFFECTS OF Q AND STRUCTURE OVER SUBREGIONAL PATHS IN WESTERN CHINA

Christopher R. Bradley and Laura E. Jones
Los Alamos National Laboratory

Sponsored by U. S. Department of Energy
Project Number: ST482A
Contract Number: W-7405-ENG-36

ABSTRACT

In order to accurately simulate the basin, crust and mantle phases generated from earthquakes and explosions, detailed knowledge of lithospheric structure is required. Inversion for velocity from crustal surface wave phases (Lg and Rg) and subsequent detailed forward modeling may be the best means of recovering three-dimensional regional and subregional structure. Simple, homogeneous three-layer (basin, crust, mantle) models of path-specific structure indicate that more complex models of the crust and upper mantle are required to perform accurate simulations. Simple velocity models are obtained via inversion or forward modeling of surface wave dispersion data from subregional paths because these phases tend to have the greatest signal to noise. After testing the models by forward modeling, models for paths with a nearly common azimuth, but at varying distances, are combined to yield two- and three-dimensional structures.

Considering moderately sized (m_b 4.5 - 6.0) earthquakes in the Lop Nor region (China) we obtain near regional to regional distance group velocity measurements. We use these to construct a family of simple, one-dimensional velocity structures for crustal, lithospheric and uppermost mantle structure in Western China and Tibet, for stations AAK, MAK, LSA and LZH. Finally, we compare results from these simple one-dimensional models with two-dimensional models incorporating basin structure and Moho topography into the original one-dimensional velocity structures.

Key Words: seismic wave propagation, crustal structure, Q

OBJECTIVE

In support of the stated goal of the Comprehensive Nuclear-Test Ban Treaty ‘to globally monitor and verify the testing of nuclear weapons’, we demonstrate the modeling of sub-regional path effects using a recently developed finite difference wave propagation algorithm. Models derived from surface wave data, gleaned from the literature, and obtained from the Cornell Database are together employed in a practical forward modeling method for determining earth structure. We thus obtain valuable insight into the physical basis for discrimination of naturally occurring earthquakes and nuclear explosions. Wave propagation modeling should be used in direct support of

- 1) the parametric study of source and propagation phenomenology along regional and sub-regional paths for earthquake and explosion sources,
- 2) analysis and accurate simulation of historic events in areas where sparse recorded data exists to test the robustness of current discrimination techniques,
- 3) the need for a quick response mechanism for discrimination of seismic events of unknown origin.

Advances in regional empirical discriminants are augmented by numerical models. Modeling can test and validate hypotheses about the basis of these discriminants. There is currently a need for information on sub-regional scales to improve discriminant models. If modeling provides information at such scales to explain the physical basis for why discriminants may work in some areas but not in others, then it is a useful tool for the analyst.

RESEARCH ACCOMPLISHED

Efforts this year have been focused in two directions: 1) developing a method for incorporating observation-based surface wave information into realistic earth models and 2) perfecting a memory efficient 3-D finite difference scheme for modeling both elastic and anelastic wave propagation over regional to subregional distances. The procedure followed includes the following steps: data selection, group velocity measurements, group velocity inversion for one-dimensional models and/or construction of composite models, initial forward modeling, and preliminary interpretation. This paper presents a first test of a new algorithm, preliminary results from our surface-wave inversion to full-waveform modeling scheme, along with a carefully selected data set to be used in future such modeling.

Data selection.

For this study, three component broadband waveforms were assembled for earthquakes recorded at IRIS stations AAK in Kyrgyzstan, MAK in Kazakhstan, and CDSN stations LSA and LZH in China between 1989 and 1996. These earthquakes are distributed across the Tien Shan fold-belt, the Tarim basin and the Tibetan plateau [Figure 1], offering source-receiver paths which cover varied and heterogeneous structure. The events are at subregional to regional distances [roughly 400 to 1400 km epicentral distance] and are of moderate size [M_b 4.5 to 6.0]. Great-circle paths shown indicate source-receiver paths for the test events modeled in this paper. Prior to further analysis, records were corrected for instrument response, rotated and decimated to one sample per second. Record sections [vertical components only] for each station are shown in Figure 2 [panels a – d]. Events modeled in this paper are shown in bold line [Figure 2a].

Group velocity measurements

Fundamental mode Rayleigh wave dispersion curves were obtained using a multiple filter scheme: a narrow band gaussian filter is applied to the displacement seismogram over many different period windows. For each period window, the maximum amplitude of the envelope function is picked. The corresponding arrival time is used to compute group velocity. We obtained group velocity measurements for a select set of vertical and radial waveforms from the above events within the period range of roughly 5 to 50 seconds, when possible. Where fundamental mode group velocity measurements for the vertical and radial components were markedly inconsistent, measurements were discarded. All measurements were made using the **PGSWMFA** [Pggplot Surface Wave Multiple Filter Analysis] software created by Chuck Ammon [St. Louis University]. Dispersion curves for each station are shown in Figure 3 [panels a – d]. Dispersion curves for AAK [panel 3a] show both the effects of propagation through the Tarim Basin [lower thickened curves] and propagation through the thickened crust of the Tien Shan. At station LSA, and to a lesser extent, station LZH [panels 3b and 3c], curves show the ‘reverse dispersion’ typical of the thickened crust.

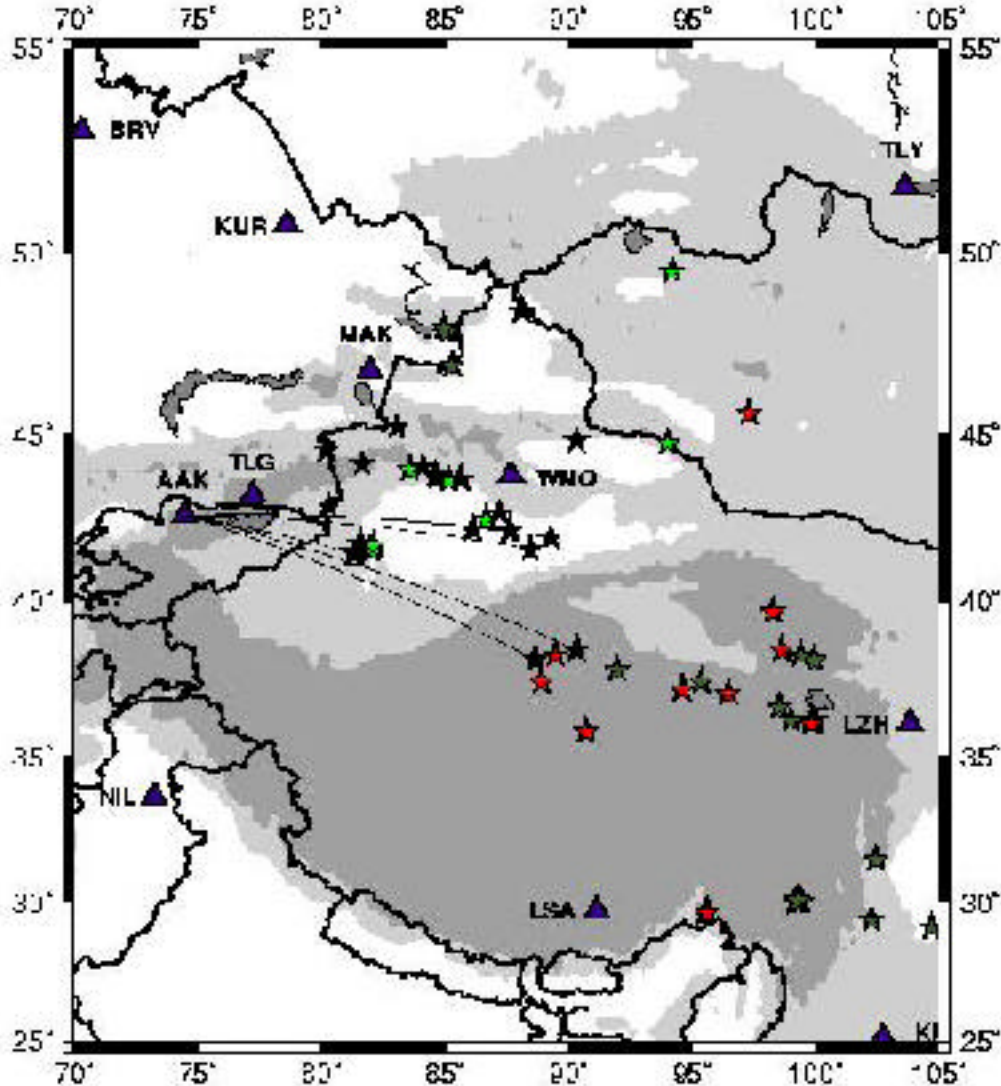


Figure 1: Map of Lop Nor area. Stations are indicated by triangles and events by stars. Solid black stars are events recorded at AAK. Paths modeled in this paper are indicated by great-circle paths.

The Tibetan Plateau. In thick grey line [panels 3b and 3c] are shown Rayleigh dispersion curves for a classic Tibetan plateau model [Romanowitz, 1982]. Dispersion at station MAK suggests the heterogeneity of the structure surrounding it [panel 3d], comprising both basin and fold-belt [Figure 1].

Preliminary Modeling

Two events were chosen to test a new numerical scheme for modeling full waveform anelastic wave propagation in three dimensions (see Appendix). These events were recorded at station AAK and propagated along similar azimuths but traveled different distances to the station. An event from 1991 May 5 (M_b 4.4) propagated 577 km across the Tarim Basin and a second event from 1993 October 2 (M_b 5.6) propagated 1300 km across a portion of the Tibetan Plateau and the Tarim Basin. Both events are shown in Figure 4 (a,b). From the group velocity analysis it is evident that the Rayleigh wave dominates the waveform beyond 175 seconds in the first event and 460 seconds in the second event. In previous studies (e.g. Jones et. al., 1997 and Bradley and Jones, 1998), modeling wave propagation across deep basins has produced a relatively weak Rayleigh wave relative to Lg. This has been attributed to crustal dispersion and high attenuation in the basins. The currently modeled events indicate a shallow source yielding a strong surface wave and higher than average crustal attenuation. Figures 4c

and 4d show the resultant synthetic seismograms from an explosion (4c) and simple double couple source. The model was developed from downloading a lithospheric cross section from the Cornell database. The velocity was adjusted using the arrival times from the actual event data. Rough estimates of Q were made based on previous studies (Bradley and Jones, 1998).

2-D Models

Figure 5a shows snapshots of the P- and S-wave field 100 seconds after the source has been initiated in a simple 3 layer crust. The parameters for the crust are:

	V _p (km/s)	V _s (km/s)	Q _p	Q _s
Basin	5.6	2.8	200	53
Crust	6.1	3.5	500	219
Mantle	7.7	4.7	1000	419

These values were partially derived from the group velocity analysis [Figure 4] and previous values from earlier modeling. From the comparison, the model under predicts the Rayleigh wave amplitude relative to L_g. This is likely due to the under estimate of Q in this edge of the Tarim Basin. Additionally, the relative strength of the Rayleigh wave indicates a source depth much shallower than the published CMT solution.

3-D Model

As a test of the new algorithm for memory efficient Q, a simple 3-D model of the subregional path from the 2 May 1991 event and AAK was constructed. The model was based on the Cornell data base cross section and extended in the orthogonal dimension symmetrically. Figure 5b shows the P- and S-wave snapshot in the xz-plane (left panel) and the vertical velocity in the xz- and xy-plane (right panel) at 45 seconds after the source initiation. The source focal mechanism is a simple in vertical strike-slip double couple. Results from this model again underestimate the Rayleigh wave amplitude due to the simplistic nature of the model/source and the potentially miss estimated focal depth.

CONCLUSIONS AND RECOMMENDATIONS:

- 1. Inversion for Layering and accurate modeling of Q:** Dispersion and scattering are required to distribute energy properly into the respective guided and surface wave modes. Surface waves provide a robust data set from which average 1-D models of velocity and Q can be inverted.
- 2. Modeling source properties can be as important as propagation:** Source depth continues to be vitally important for accurately modeling surface wave phases. Source mechanism and depth can be modeled and improved upon via faster techniques than finite difference, then the improved focal mechanism used in the full waveform modeling.
- 3. Fast numerical approximation of Q is a necessary component:** With the realization that 3-D propagation effects are important to the simulation, we find that intrinsic attenuation and scattering are required for accurate modeling. Memory restrictions on most computers require a better method of simulating attenuation. Coarse graining of memory variables used in Q simulation provide this method.

Our future modeling will include more accurate source descriptions, the more memory efficient “coarse grained Q” method and composite velocity models of 1-D (derived from surface wave inversions) and 3-D models (derived from whole earth data set like those in the Cornell data base statistical parameters inverted from coda and topography).

Appendix:

Memory Efficient Finite Difference Modeling of Intrinsic Attenuation (Q):

Finite difference (FD), finite element (FE), and pseudospectral methods are currently able to solve transient three-dimensional seismic wave propagation problems over domains sufficiently large that anelastic attenuation should not be neglected. Realistic treatment of anelastic losses is especially important for simulating the earthquake-induced response of complex geologic structures such as sedimentary basins (e.g., Frankel and Vidale, 1992; Yomogida and Etgen, 1993; Olsen and Archuleta, 1996; Wald and Graves, 1998; Pitarka et al, 1998; Sato et al., 1999). An important component of the ground motion in basins is the trapping of incident

waves at the basin edges, resulting in the excitation of surface waves in the basin sediments (e.g., Field, 1996). These basin-edge induced waves in turn may reverberate within the basin. Numerical simulations which neglect anelastic losses in the sediments may seriously overpredict the amplitude and duration of the ground motion, even if the seismic velocity structure and source are well-modeled. Realistic formulation of anelastic losses is also important in other applications of 3D numerical simulations. These include studies directed at seismic verification of the comprehensive nuclear test ban treaty, modeling of seismic reflection profiles, and global-scale seismic waveform modeling.

In this appendix, we extend the coarse-grained memory variable approach to anelastic wave propagation in three dimensions. We implement the method in a fourth-order finite difference program, demonstrate its accuracy for plane P and S waves. We also outline the extension of the method to power law frequency-dependent Q .

Implementation for acoustic case.

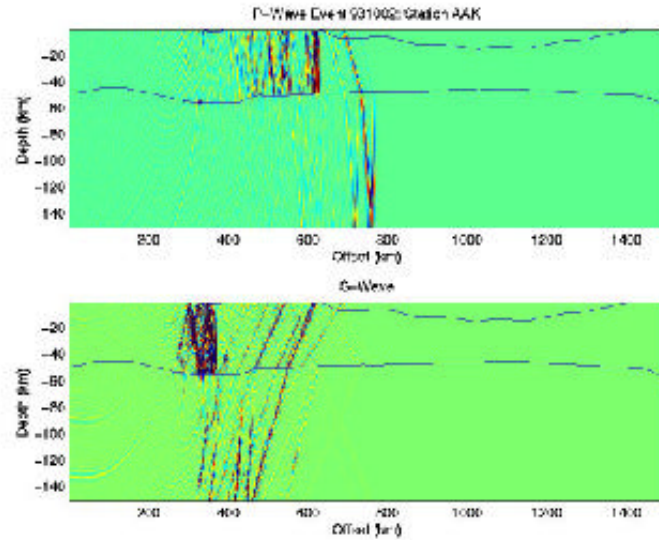
Day, 1998 also gave a practical implementation of coarse graining for the acoustic wave equation discretized on a 3D lattice. To approximate the special case of frequency-independent Q , equally spaced on a logarithmic scale, between lower and upper absorption-band cutoffs. All weights w_k were set to 1. In the acoustic case, the appropriate modulus is the bulk modulus and the bulk modulus relaxation is set such that the specified Q value, Q_0 , will be realized at some prescribed reference frequency (near the center of the absorption band). The appropriate Q is then that which satisfies

$$Q_0^{-1} = \frac{\pi \delta \kappa}{2 \kappa_u} \ln \frac{\tau_M}{\tau_m} + \frac{\delta \kappa}{\kappa_u} \ln(\omega_0 \tau_m)^{-1}.$$

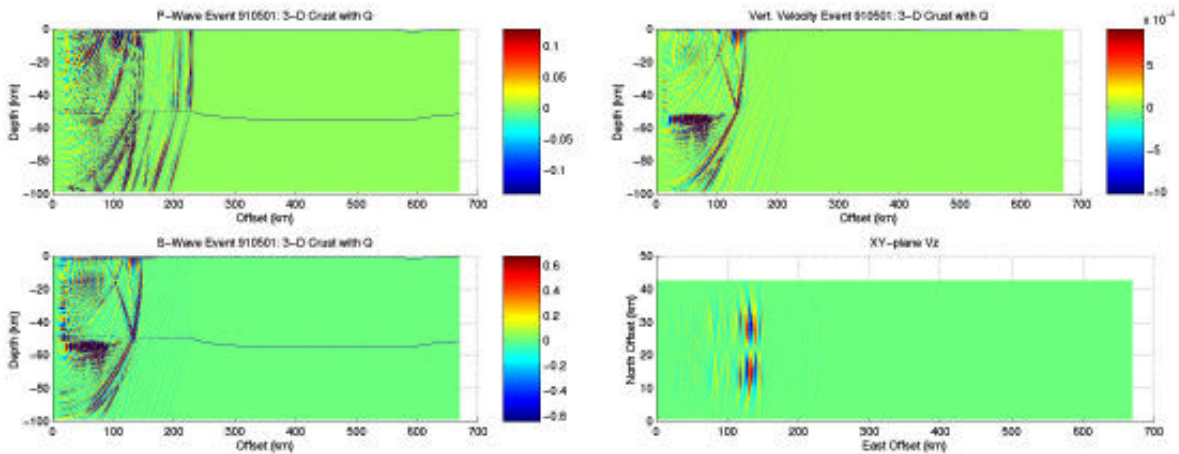
This procedure successfully simulates frequency-independent Q , to within 3% tolerance, over 2 orders of magnitude in frequency, yet requires only 1 memory variable per stress node. A limitation of the method is that it produces strong scattering at wavelengths shorter than 4 grid cells (as predicted by the perturbation analysis, and confirmed by numerical experiments). As a result, the method is probably most appropriate for use with low-order finite difference and finite element methods, for which wavelengths shorter than 4 grid cells are already subject to large errors due to numerical dispersion. On the basis of acoustic wave tests, the method appears to be well suited to the fourth-order staggered-grid finite difference method which is now widely used in seismological applications.

ANELASTIC FORMULATION

The coarse grained approach is easily generalized for anelastic models, and the generalization is particularly simple for isotropic anelasticity, to which we limit ourselves here. In the isotropic case, the stress strain relationship can be partitioned into separate relationships for, respectively, the mean stress (in terms of the volumetric strain and a volumetric memory variable), and the deviatoric stresses σ_{ij} (in terms of the deviatoric strains ϵ_{ij} and corresponding memory variables). Considering that only 5 of the 6 deviatoric stress (and strain) components are independent, this formulation leads to one equation for each of 6 memory variables. For example, adding attenuation to a 3D staggered grid FD method (assuming a conventional velocity-stress formulation, e.g., Graves, 1996) requires adding 6 memory variables (one for each stress component) to each unit cell of the grid.



5a)



5b)

Figure 5. In 5a are shown a snapshots of the P- and S-wave field at 100 seconds after initiation of a double couple source for a simple crustal model between AAK and an earthquake 1300 km away. Figure 5b shows the snapshots from a full 3-D computation for the subregional path from the 2 May 1991 event to AAK.

In the above formulation, one could assign different frequency dependence to the compressional and shear Q 's. This would be accomplished by using one set weights in the equation controlling the memory variable for mean stress, and a different set in the 5 equations controlling the memory variables associated with the deviatoric stresses. The development is less cumbersome, however, if we make the additional assumption that the Q_s share a common frequency dependence. One advantage of this simplification is that we can avoid partitioning the stress tensor into mean-stress and deviatoric-stress parts. Instead, we form linear combinations of the mean-stress and deviatoric-stress memory variables, choosing combinations that correspond to the usual physical components of the total stress tensor. The above procedure leads to the following set of equations

$$\sigma_{ij} = 2\mu_u \varepsilon_{ij} + \left(\kappa_u - \frac{2}{3} \mu_u \right) \varepsilon_{kk} - \xi_{ij}, \quad \text{and}$$

$$\tau \frac{d\xi_{ij}}{dt} + \xi_{ij} = w \left[2\mu_u A_s \varepsilon_{ij} + \left[\left(\kappa_u + \frac{4}{3} \mu_u \right) A_p - 2\mu_u A_s \right] \varepsilon_{kk} \delta_{ij} \right],$$

where A_p and A_s are constants that scale with Q_p^{-1} and Q_s^{-1} , respectively. For the special case of frequency-independent Q , these constants are

$$A_p = \frac{2}{\pi} Q_p^{-1} \ln \frac{\tau_M}{\tau_m} \left[1 - \frac{2}{\pi} Q_p^{-1} (\ln \omega_0 \tau_m) \right]^{-1}, \quad \text{and}$$

$$A_s = \frac{2}{\pi} Q_s^{-1} \ln \frac{\tau_M}{\tau_m} \left[1 - \frac{2}{\pi} Q_s^{-1} (\ln \omega_0 \tau_m) \right]^{-1}.$$

STAGGERED-GRID FINITE DIFFERENCE IMPLEMENTATION

We incorporate the anelastic coarse graining in a 3D staggered-grid FD method. The implementation is analogous that used in Day, 1998, for the acoustic case. The underlying elastodynamic code, that of Olsen (1994), approximates spatial derivatives with fourth-order accuracy and time derivatives with second-order accuracy (Graves, 1996, gives a detailed description of the difference equations). Figure 5b shows the result of a subregional test of the 3-D finite difference code with attenuation calculated via coarse graining.

REFERENCES:

- Bradley, C. and Jones, E., Modeling propagation effects from explosions in western China and India, 20th Annual Seismic Research Symposium on Monitoring a CTBT, Santa Fe, NM, 1998.
- Bradley, C. and Day, S., Elastic Coarse-Graining of Memory Variables: Memory efficient Q simulation for finite difference methods. *Bull. Seis. Soc. Am.*, (in Prep), (LA-UR-99-719) 1999.
- Day, S., Efficient simulation of constant Q using coarse-grained memory variables. *Bull. Seism. Soc. Am.*, 88(4) 1051-1062, 1998.
- Day, S., and Minster, B., Numerical simulation of attenuated wavefields using a Padé approximant method, *Geophysical J. Roy. Astr. Soc.*, 78, 105-118, 1984.
- Dziewonski, A., Bloch, A., and Landisman, M., A technique for the analysis of transient seismic signals, *Bull. Seism. Soc. Am.*, 59(1), 427-444, 1969.
- Field, E.H. (1996). Spectral amplification in a sediment-filled valley exhibiting clear basin-edge-induced waves, *Bull. Seism. Soc. Am.* 86, 991-1005.
- Frankel, A., and J. Vidale (1992). A three-dimensional simulation of seismic waves in the Santa Clara Valley, California, from a Loma Prieta aftershock, *Bull. Seism. Soc. Am.* 82, 2045-2074.
- Jones, E., Bradley, C., App, F., Bos, R., and Patton, H., Modeling seismic propagation from large scale structural features in western China. LANL Memorandum, LA-UR-97-4186, 1998.
- Kosarev, G., Petersen, N., Vinnik, L., and Roecker, S., Receiver functions for the Tien Shan analog broadband network: Contrasts in the evolution of structure across the Talasso-Fergano fault. *J. Geophys. Res.*, 98(3), 4437-4448, 1993.
- Olsen, K.B. (1994). Simulation of three-dimensional wave propagation in the Salt Lake Basin, *Ph.D. Thesis*, University of Utah, Salt Lake City, Utah, 157 pp.
- Olsen, K.B., and R.J. Archuleta (1996). Three-dimensional simulation of earthquakes on the Los Angeles fault system, *Bull. Seism. Soc. Am.* 86, 575-596.

- Mahdi, H., and Pavlis, G., Velocity variations in the crust and upper mantle beneath the Tien Shan inferred from Rayleigh wave dispersion: Implications for tectonic and dynamic processes. *J. of Geophys. Res.*, 103(B2) 2693-2703, 1998.
- Pitarka, A., K. Irikura, T. Iwata, and H. Sekiguchi (1998). Three-dimensional simulation of the near-fault ground motion for the 1995 Kyogo-ken Nanbu (Kobe), Japan, earthquake, *Bull. Seism. Soc. Am.*, 88, 428-440.
- Romanowitz, B., Constraints on the structure of the Tibet Plateau from pure path phase velocities of Love and Rayleigh waves. *J. of Geophys. Res.*, 87(B8), 6865-6883, 1982.
- Sato, T., R.W. Graves, and P.G. Somerville (1999). Three-dimensional finite-difference simulations of long-period strong motions in the Tokyo metropolitan area during the 1990 Odawara Earthquake (M_j 5.1) and the Great 1923 Kanto Earthquake (M_s 8.2) in Japan, *Bull. Seism. Soc. Am.* 89, 579-607.
- Wald, D.J., and R.W. Graves (1998). The seismic response of the Los Angeles basin, California, *Bull. Seism. Soc. Am.* 88, 337-356
- Yomogida, K., and J.T. Etgen (1993). 3D wave propagation in the Los Angeles Basin for the Whittier-Narrows earthquake, *Bull. Seism. Soc. Am.* 83, 1325-1344.

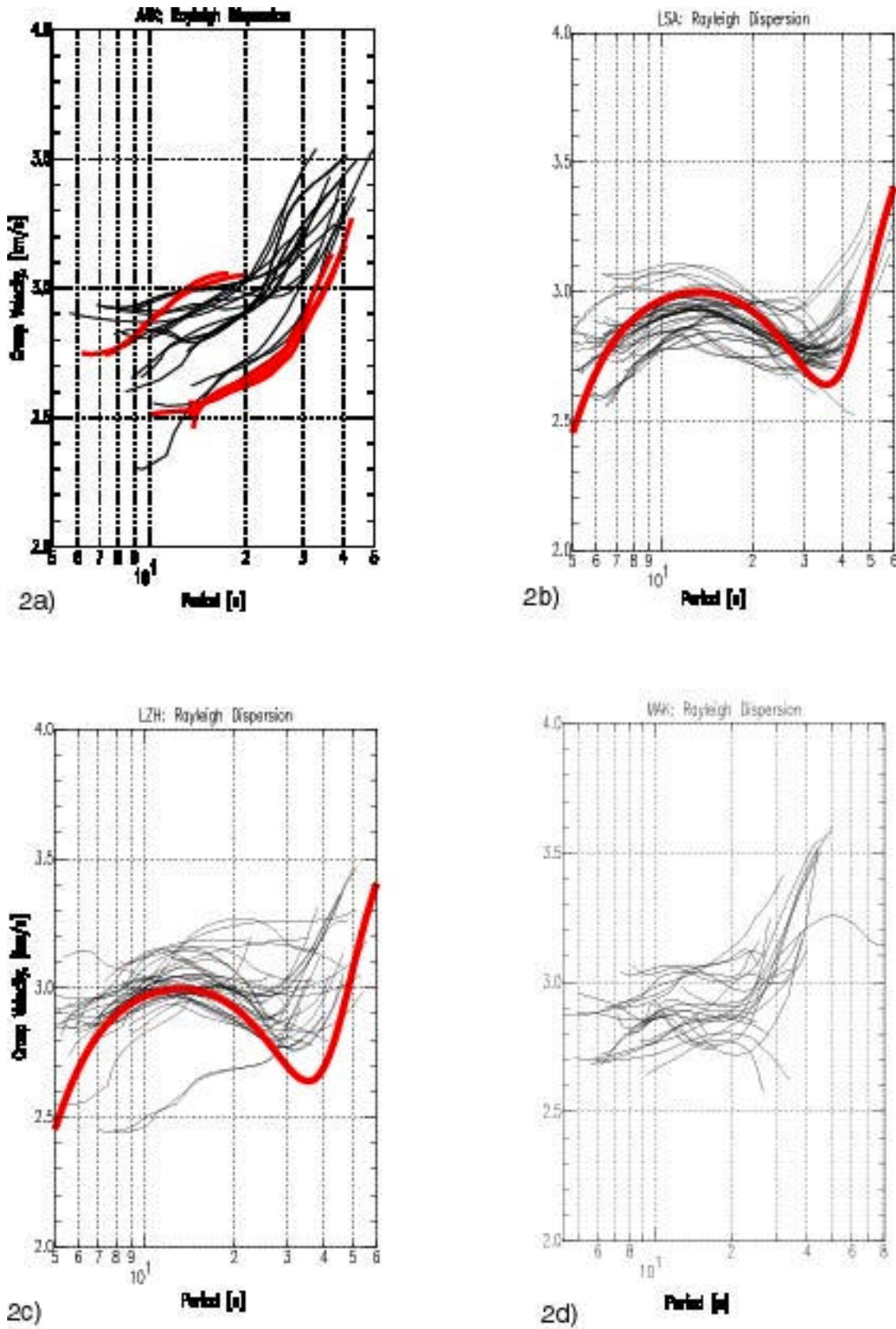
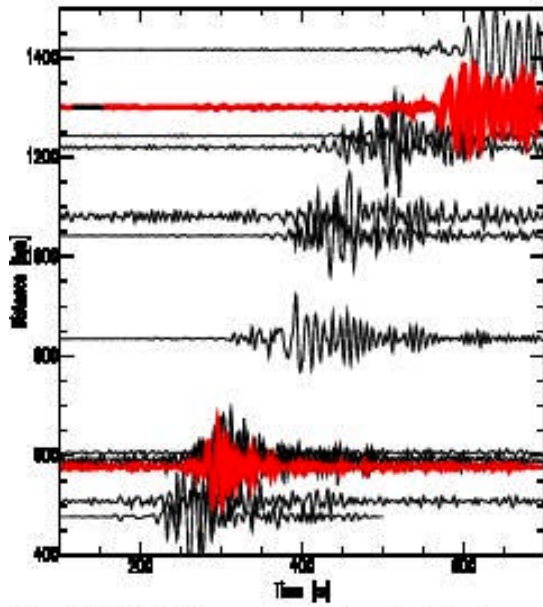
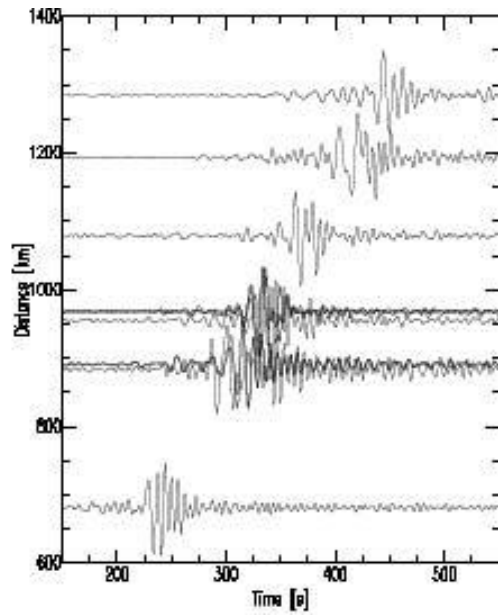


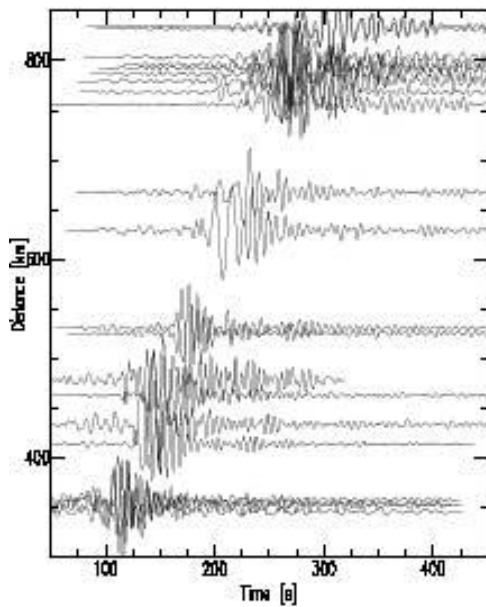
Figure 2) Rayleigh dispersion for stations AAK, LSA, LZH, and MAK.



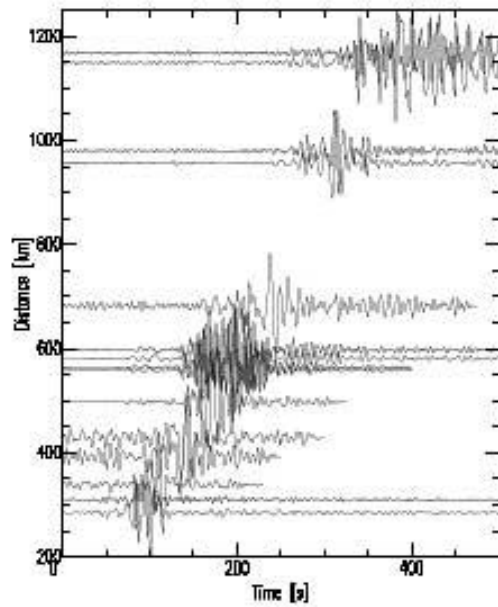
3a) AAK BHZ [Low pass filtered at 5 s]
Records modeled in this paper are shown in thick grey line.



3b) LSA BHZ [Lowpassed]



3c) LZH BHZ [Lowpassed]



3d) MAK BHZ [Lowpassed]

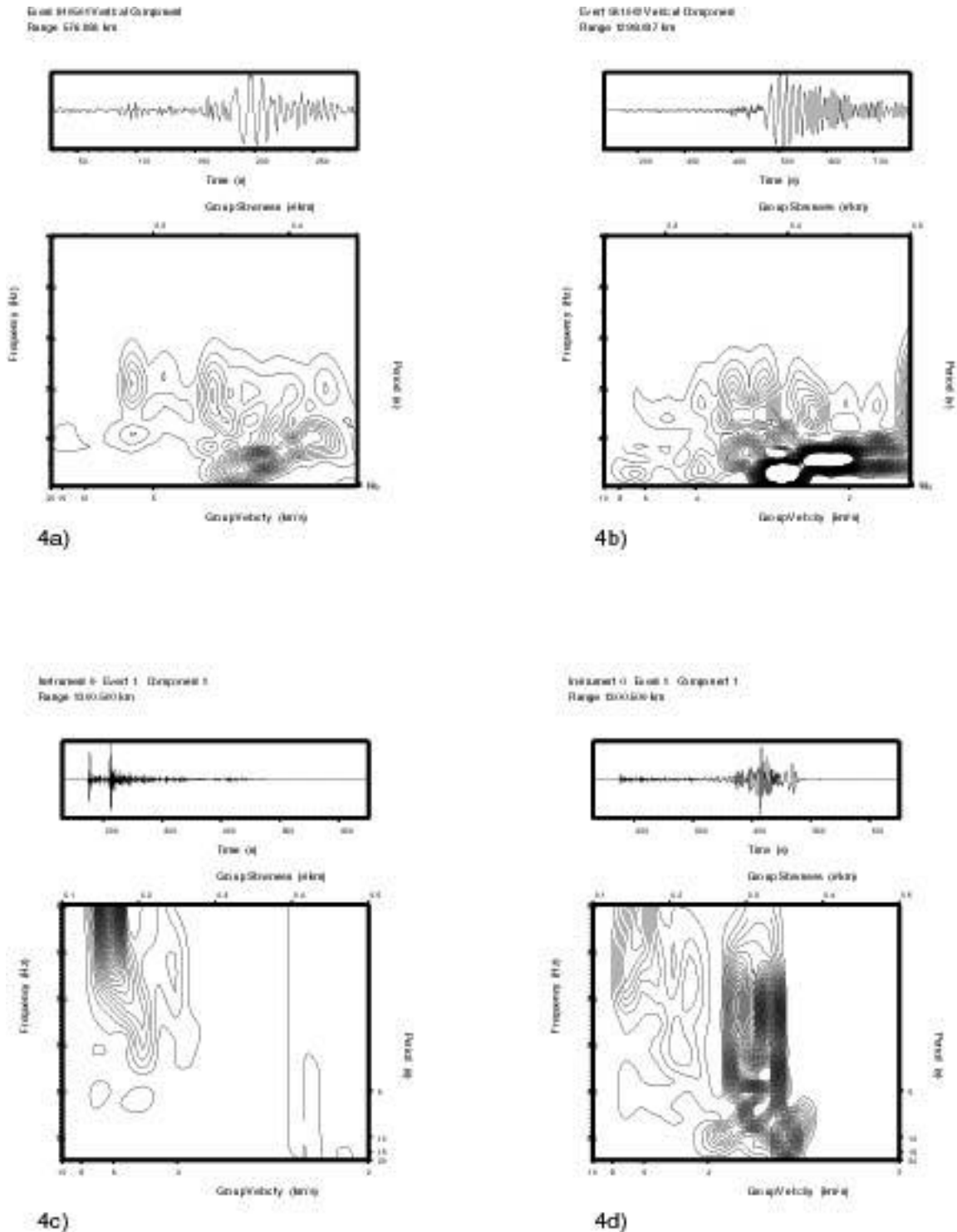


Figure 4. 4a) is a data and group velocity plot from an earthquake at 577 km from station AAK. The Rayleigh wave phase is the dominant arrival. Similarly, in 4b) are shown the data and group velocity plot for an earthquake at similar azimuth but at a range of 1298 km. Figures 4c and 4d are the resultant seismograms from a simple 2-D crust with attenuation for an explosion source and moment tensor respectively.